ACS APPLIED MATERIALS & INTERFACES

Research Article

www.acsami.org

Polymeric Nanomedicine for Tumor-Targeted Combination Therapy to Elicit Synergistic Genotoxicity against Prostate Cancer

Qingqing Yang,[†] Yang Yang,[†] Lian Li, Wei Sun, Xi Zhu, and Yuan Huang*

Key Laboratory of Drug Targeting and Drug Delivery System, Ministry of Education, West China School of Pharmacy, Sichuan University, No. 17, Block 3, Southern Renmin Road, Chengdu 610041, People's Republic of China

Supporting Information

ABSTRACT: To improve the therapeutic efficacy of anticancer combination therapy, we designed a nanoplatform based on *N*-(2-hydroxypropyl) methacrylamide (HPMA) copolymers that allows covalent bonding of two chemotherapeutics acting via different anticancer mechanisms and that can enter target cells by receptor-mediated endocytosis. Doxorubicin (DOX) was covalently conjugated to a nanosized HPMA copolymer using a pH-sensitive hydrazone bond and 5-fluorouracil (5-Fu) was conjugated to the same backbone using an enzymatically degradable oligopeptide Gly-Phe-Leu-Gly sequence. Then, the conjugate was decorated with galectin-3 targeting peptide G3-C12 [P-(G3-C12)-DOX-Fu]. The two drugs showed similar in vitro release profiles, suggesting that they may be able to work synergistically in the codelivery system. In galectin-3 overexpressed PC-3 human prostate carcinoma cells, P-(G3-C12)-DOX-Fu surprisingly exhibited comparable cytotoxicity to free DOX at high concentration by increasing cell internalization and exerting synergistic genotoxic effects of cell cycle arrest, caspase-3 activation, and DNA damage. In mice bearing PC-3 tumor xenografts, the use of tumor-targeting ligand substantially enhanced the intracellular delivery of P-(G3-C12)-DOX-Fu in tumors. The targeted dual drug-loaded conjugate inhibited tumor growth to a greater extent (tumor inhibition of 81.6%) than did nontargeted P-DOX-Fu (71.2%), P-DOX (63%), DOX·HCl (40.5%), P-Fu (32.0%), or 5-Fu (14.6%), without inducing any obvious side effects. These results demonstrate the potential of synergistic combination therapy using targeted nanocarriers for efficient treatment of prostate cancer.

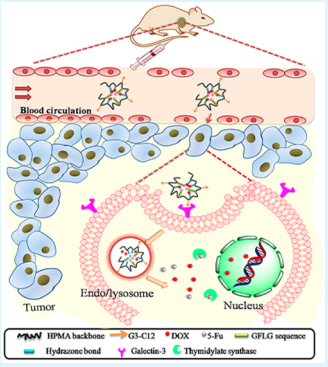

KEYWORDS: *combination therapy, prostate cancer, HPMA copolymer, G3-C12, synergistic genotoxicity*

INTRODUCTION

Combination therapy is increasingly used as a primary cancer treatment regimen to avoid the poor response and resistance often associated with monotherapy.[1,2] However, the traditional mode of combination therapy by simply applying drug cocktail often shows limited efficacy because the two drugs do not have overlapping pharmacokinetics or tissue distribution, and circulation of free drugs in the body increases the risk of side effects.[3] Advances in nanotechnology have opened up unprecedented opportunities for combination therapy by enabling temporally and spatially controlled delivery of encapsulated drugs.[4−9] Loading nanocarrier platforms such as liposomes[5] and nanoparticles[6] with multiple therapeutic agents can enhance overall therapeutic efficacy with lower doses and better safety. However, most of these approaches are based on noncovalent drug encapsulation, resulting in poor stability and batch-to-batch variability in drug loading and release kinetics, especially when the two drugs possess different physicochemical properties.[7]

Water-soluble polymer-drug conjugates, such as drug-conjugated *N*-(2-hydroxypropyl) methacrylamide (HPMA) copolymers, have emerged as promising therapeutic nanocarriers for cancer treatment owing to their unique properties, such as enhanced drug solubility, improved pharmacokinetic behavior, and increased tumor accumulation mediated by the enhanced permeability and retention (EPR) effect.[10−12] By manipulating the ratio and functionality of the monomers, the loading and release of covalently conjugated drugs from HPMA copolymers can be precisely controlled.[13] Recently, HPMA copolymer−drug conjugates have shown distinct advantages for combination therapy in several studies.[14−18] Krakovicova et al. developed HPMA copolymers containing the anti-inflammatory and antiproliferative drug dexamethasone and the anticancer drug doxorubicin (DOX) on account of that dexamethasone may act as a chemosensitizer in cancer chemotherapy.[14] Excellent synergistic anticancer activity of the dual drug-loaded conjugate was observed over single drug loaded-conjugates against dexamethasone-sensitive B-cell lymphoma.[15] Lammers et al. conjugated gemcitabine and DOX onto one HPMA copolymer, and the conjugate containing both drugs inhibited angiogenesis and induced apoptosis more remarkably than did the combination of two copolymer conjugates each bonding a single drug.[16] Furthermore, Kopeček et al. found that combination of two copolymer−drug conjugates containing the chemotherapeutic agent docetaxel and the hedgehog pathway inhibitor cyclopamine could kill

Received: December 30, 2014
Accepted: March 16, 2015
Published: March 16, 2015

DOI: 10.1021/am509204u
ACS Appl. Mater. Interfaces 2015, 7, 6661−6673

cancer stem cells and bulk tumor cells more effectively than either conjugate alone.[17] This is because the hedgehog pathway is not only involved in prostate cancer progression but also critical in promoting prostate cancer stem cells self-renewal and growth.[19] In a recent study, Kostkova el al. designed biodegradable high molecular weight (MW) diblock HPMA copolymers (76 kDa) for codelivery of anticancer antibiotic mitomycin C and DOX with different mechanisms of action. In vivo studies confirmed the therapeutic benefit of this combination strategy based on high MW polymer.[18] Because HPMA polymer-based combination therapy with dual drug in one polymer chain can provide more accurate dose optimization and align the biodistribution of the combined drugs,[20,21] this strategy might be superior to the single drug loaded conjugates or the combination of two individual polymeric prodrugs.

Despite these advantages, HPMA polymer presents a substantial drawback: its poor cell membrane affinity means that it does not internalize efficiently into cells even after accumulating in tumor tissue.[22,23] Alternatively, active targeting attempts to overcome this dilemma by decorating HPMA polymers with peptides or other ligands that recognize tumor-specific receptors.[24] Galectin-3 is a member of β-galactoside-binding proteins and is overexpressed on prostate carcinoma cells.[25] We have shown that covalently attaching galectin-3 targeting peptide G3-C12 (sequence: ANTPCGPYTHDCPVKR) to HPMA polymers leads to significantly greater cell uptake relative to untargeted HPMA polymers and exhibits excellent potential for targeting prostate tumors in vivo.[26,27]

The topoisomerase II inhibitor DOX can induce irreversible single- and double-stranded DNA breaks during transcription and replication.[28] The thymidylate synthase inhibitor 5-fluorouracil (5-Fu) was recently reported to selectively destroy tumor-associated myeloid-derived suppressor cells and thereby promote T cell-dependent antitumor responses.[29] In clinical use, both drugs are often combined with other chemotherapeutics (e.g., cyclophosphamide or mitomycin-C) to treat breast and pancreatic carcinoma,[30,31] but few attempts have been made to deliver DOX and 5-Fu in a single vehicle to produce synergistic genotoxicity or to minimize their adverse effects when used individually.

In the present study, the codelivery of DOX and 5-Fu using G3-C12 modified HPMA copolymers for prostate cancer therapy was developed. To maintain the integrity of the nanocarrier in the blood circulation and induce specific drug release in the tumor cell, DOX and 5-Fu were conjugated to a single HPMA polymer chain via a pH-sensitive hydrazone bond[32] and an enzymatically degradable glycylphenylalanylleucylglycine (GFLG) tetrapeptide spacer, respectively.[26] The synchronized release of both drugs in response to enzyme activity and acidity in the endo/lysosomal compartment of cancer cells might be achieved. We hypothesized that EPR-mediated targeting of the nanovehicle could direct both pendant drugs into the tumor tissue at the same time, while G3-C12 modification of HPMA copolymers would enhance their intracellular internalization (Scheme 1). The potency of this targeted codelivery system was evaluated in galectin-3 overexpressed PC-3 human prostate carcinoma cells and in mice bearing PC-3 tumor xenografts. It was expected that the targeted combination therapy would promote synergistic anticancer efficacy.

Scheme 1. Schematic Illustration of Tumor Targeting, Internalization, And Synergistic Genotoxicity by HPMA Copolymer Conjugates Loaded with Both 5-Fluorouracil and Doxorubicin and Decorated with G3-C12 Peptide That Binds Galectin-3[a]

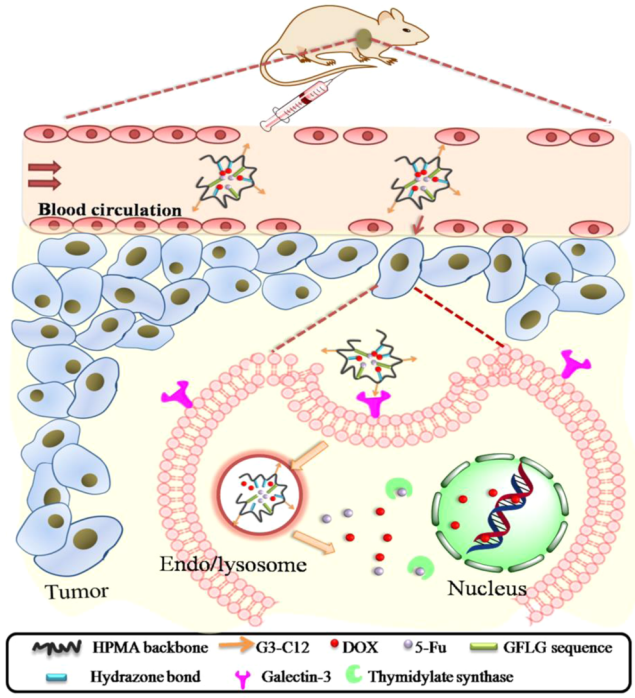

[a]This polymeric nanovehicle is called P-(G3-C12)-DOX-Fu in the text.

EXPERIMENTAL SECTION

Materials. 5-Fluorouracil was purchased from Nantong Pharmaceutical Co., Ltd. (Jiangsu, China). Doxorubicin hydrochloride (DOX·HCl) was purchased from Dalian Meilun Biotech Co., Ltd. (Shandong, China). The galectin-3 binding peptide G3-C12 (sequence: ANTPCGPYTHDCPVKR) was synthesized by Kaijie Biopharm Co., Ltd. (Sichuan, China). Scrambled peptide S-G3-C12 (sequence: PTHVTCKYCPAGNRPD) was synthesized by GL Biochem Co., Ltd. (Shanghai, China). The following reagents were purchased from Sigma-Aldrich (St. Louis, MO): 3-(4,5-dimethyl- 2-tetrazolyl)-2,5-diphenyl-2H tetrazolium bromide (MTT), 4′,6-diamidino-2-phenylindole (DAPI), papain, cathepsin B, RNase A, propidium iodide (PI), and SYBR Green dye. *N*-(2-Hydroxypropyl) methacrylamide (HPMA),[33] *N*-methacryloyl-glycylglycyl-hydrazide-doxorubicin (MA-GG-NHN=DOX),[34] *N*-methacryloyl-glycylglycyl-pnitrophenyl ester (MA-GG-ONp),[35] *N*-methacryloyl-glycylphenylalanylleucylglycine (MA-GFLG−OH),[33] and 1,3-dimethylol-5-fluorouracil[36] were synthesized according to previous reports. All other reagents and solvents were purchased from Aladdin Reagent Co., Ltd. (Shanghai, China) and used as received.

Synthesis of HPMA Copolymer−Drug Conjugates. Conjugates containing both doxorubicin and 5-fluorouracil (P-DOX-Fu) were synthesized in two consecutive steps. First, the copolymer precursor for loading DOX (P-DOX−OH) was prepared by random radical precipitation copolymerization in an acetone/dimethyl sulfoxide (DMSO) mixture (AIBN, 2 wt %; monomer concentration, 12.5 wt %; molar ratio HPMA/MA-GG-NHN=DOX/MA-GFLG−OH, 82.5:7.5:10; 50 °C; 24 h).[37] Then, solvent was removed by rotary evaporation. The remaining polymerization mixture was dissolved in methanol, and the polymer precursor was further isolated by precipitation into diethyl ether. Second, 1,3-dimethylol-5-fluorouracil and P-DOX−OH were dissolved in acetonitrile/dimethylformamide (DMF) (5:12, v/v), after which *N*,*N*-dicyclohexylcarbodiimide (DCC)

DOI: 10.1021/am509204u
ACS Appl. Mater. Interfaces 2015, 7, 6661−6673

was added, and the mixture was stirred for 18 h at room temperature. The copolymer was purified by gel filtration on a Sephadex G-25 column using double distilled water as eluent and was obtained by freeze-drying.

The final HPMA copolymer conjugates loaded with both DOX and 5-Fu, and decorated with galectin-3 binding peptide G3-C12 [P-(G3-C12)-DOX-Fu] were synthesized, as shown in Figure 1A. In the first step, the copolymer precursor containing DOX and active ester (P-DOX-ONp) was prepared by random radical precipitation copolymerization in an acetone/DMSO mixture using AIBN as initiator. Then, 1,3-dimethylol-5-fluorouracil was conjugated to P-DOX-ONp as mentioned above (P-DOX-Fu-ONp). Finally, G3-C12 peptide was attached to P-DOX-Fu-ONp by substituting terminal p-nitrophenyl group (ONp) of the nondegradable dipeptide glycylglycine. Briefly, P-DOX-Fu-ONp and G3-C12 were dissolved in DMF (molar ratio ONp/G3-C12, 1:1). The reaction mixture was stirred at room temperature for 20 h and then purified by dialysis against distilled water for 24 h at 4 °C. The resulting solution was finally lyophilized to obtain P-(G3-C12)-DOX-Fu.

To enable comparison of the activity of dual drug-loaded HPMA copolymer conjugates with that of single drug-loaded conjugates, we synthesized HPMA copolymer-doxorubicin conjugates (P-DOX)[34] and HPMA copolymer-5-fluorouracil conjugates (P-Fu)[38] by radical copolymerization according to established procedures.

Characterization of HPMA Copolymer−Drug Conjugates. The molecular weight and polydispersity index (PDI) of the conjugates were determined based on a HPMA homopolymer calibration using an AKTA Fast Protein Liquid Chromatography (FPLC) system [GE Healthcare Life Sciences; Superose 6 10/300GL analytical column; mobile phase, phosphate buffer (pH 7.4)] equipped with UV and refractive index detectors. An aliquot of the polymer precursor (P-DOX-ONp) was hydrolyzed with 0.1 M sodium hydroxide (NaOH) to enable the determination of the released p-nitrophenol (ONp) using UV−vis spectroscopy at 400 nm. To measure the 5-Fu content, HPMA copolymer-drug conjugates were hydrolyzed in NaOH solution (0.1 M) at 37 °C for 20 min to release 5-Fu, and then the solution was neutralized using hydrochloric acid (HCl) solution (0.5 M). A method based on high-performance liquid chromatography (HPLC) was used to assay 5-Fu content (Agilent Technologies 1200 Series; Dikma Diamonsil C18 column 250 × 4.6 mm, 5 μm; mobile phase, distilled water; wavelength, 267 nm). The content of DOX was measured by UV−vis spectroscopy using ε_{488} = 9860 L mol^{-1} cm^{-1} (water). The amount of G3-C12 attached to polymers was determined by amino acid analysis (Commonwealth Biotech, Richmond, VA). The size distribution [hydrodynamic radius (R_h)] and zeta potential of nanocarriers in deionized water were measured on a Malvern Zetasize NanoZS90 instrument (Malvern Instruments Ltd., Malvern, United Kingdom). The morphology of P-(G3-C12)-DOX-Fu was observed by a transmission electron microscopy (FEI Tecnai GF20S-TWIN, Hillsboro, OR).

In Vitro Drug Release. The release of DOX from the polymer conjugates [P-DOX, P-DOX-Fu, and P-(G3-C12)-DOX-Fu; polymer concentration equivalent to 0.5 mM DOX] was measured by incubating the conjugate at 37 °C for 48 h in phosphate buffers at pH 5.0 or 7.4 (adjusted using 0.1 M phosphate buffer containing 0.05 M NaCl). At predetermined time points, the content of DOX released from polymer conjugates was determined after its extraction from the incubation media into chloroform. Briefly, a mixture of polymer solution (0.1 mL) and buffer (0.2 M Na_2CO_3/$NaHCO_3$, pH 9.8, 0.3 mL) was extracted with chloroform (0.8 mL).[39] The organic layer was separated and dried under nitrogen. The resulting residue was dissolved in mobile phase and analyzed by HPLC [mobile phase, methanol/acetonitrile/0.01 M ammonium dihydrogen phosphate/glacial acetic acid (50:22:28:0.5, v/v); wavelength, 488 nm]. The release of 5-Fu from the polymer conjugates [P-Fu, P-DOX-Fu, and P-(G3-C12)-DOX-Fu] was investigated by incubating the conjugates in McIlvaine's buffer [50 mM citrate/0.1 M phosphate; 2 mM ethylene diamine tetraacetic acid (EDTA), pH 6.0] at 37 °C for 48 h in the presence of papain (2 μM)[40] or cathepsin B (0.5 μM)[41] or in phosphate buffer (0.1 M, pH 7.4). At predetermined time points, a sample was withdrawn and analyzed by HPLC system. All determinations were carried out in triplicate.

Cell Culture. PC-3 human prostate carcinoma cells were purchased from the Chinese Academy of Science Cell Bank for Type Culture Collection (Shanghai, China) and cultured in Dulbecco's modified Eagle's medium (DMEM)/F12 medium (Gibco) supplemented with 10% fetal bovine serum (Hyclone) and 1% penicillin−streptomycin (Hyclone) at 37 °C in a 5% CO_2 atmosphere. All experiments were performed on cells in the logarithmic growth phase.

Endocytic Uptake Analysis. For studies of cell uptake by confocal microscopy, PC-3 cells were grown on sterile coverslips in a 6-well plate (Corning, Inc., Corning, NY) and incubated for 24 h. The medium was then replaced with medium containing P-DOX, P-DOX-Fu or P-(G3-C12)-DOX-Fu (equivalent to 5 μg/mL of DOX) in the presence or absence of free G3-C12 peptide (200 nM). After 2 h of incubation, cells were washed with phosphate-buffered saline (PBS) and fixed using 4% paraform solution. Ten minutes before imaging, DAPI was added to visualize the nuclei. Coverslips were mounted on the glass slides with a drop of antifade mounting medium and visualized under a confocal laser scanning microscope (LSM 510 DUE, Carl Zeiss, Jena, Germany). For flow cytometric analysis, PC-3 cells were cultured in 12-well plates and incubated for 24 h. Then, the cells were incubated for 2 h with P-DOX, P-DOX-Fu, or P-(G3-C12)-DOX-Fu (equivalent to 1, 5, or 10 μg/mL of DOX) in the presence or absence of free G3-C12 peptide (200 nM). After incubation, cells were harvested, washed with PBS, and then analyzed by flow cytometry (Cytomics FC 500, Beckman Coulter Ltd.). Cells (1.0×10^4) were collected, and their mean fluorescence intensity was recorded. A scrambled version of G3-C12 (S-G3-C12, PTHVTCKYCPAGNRPD) was synthesized. The scrambled peptide S-G3-C12 was conjugated to the dual drug-loaded HPMA polymer conjugates, namely P-(S-G3-C12)-DOX-Fu. Flow cytometry was used to assess endocytic uptake of P-DOX, P-DOX-Fu, P-(G3-C12)-DOX-Fu, and P-(S-G3-C12)-DOX-Fu in the presence or absence of free S-G3-C12 peptide (200 nM) after 2 h of incubation with PC-3 cells as mentioned above (equivalent to 5 μg/mL of DOX).

In Vitro Cytotoxicity. Cytotoxicity was assessed using a tetrazolium dye (MTT) assay based on the reduction of the MTT formazan crystals by living cells. PC-3 cells were seeded on 96-well plates at a density of 8×10^3 cells/well, and cultured for 24 h. Subsequently, cells were incubated with free 5-Fu, DOX or conjugates at different concentrations (equivalent to 1−70 μg/mL of DOX and 0.62−43.4 μg/mL of 5-Fu). After 12 h of incubation, the medium was removed and cells were washed with PBS. Then, cells were incubated with fresh medium for another 24 h at 37 °C. Afterward, the cells were incubated with MTT dye for 4 h. Then, the medium was removed before adding DMSO (150 μL) to each well to dissolve the formazan precipitate, and absorbance was measured at 570 nm using a plate reader (Varioskan Flash, Thermo, Waltham, MA). Untreated cells were used as a control, and the viability was expressed as the percentage of the absorbance of the control. IC_{50} values (μg/mL) were calculated using SPSS software (IBM, Chicago). The synergistic, additive, or antagonistic cytotoxic effects were evaluated using the combination index (CI), which was based on the Chou−Talalay method and the following equation: $CI_x = [(D)_1/(D_x)_1] + [(D)_2/(D_x)_2]$. $(D_x)_1$ and $(D_x)_2$ represent the IC_x value of drug 1 alone and drug 2 alone, respectively. $(D)_1$ and $(D)_2$ represent the concentration of drugs 1 and 2 in the combination system at the IC_x value.

For experiments with multicellular tumor spheroids, PC-3 cells were seeded onto a 96-well plate (Corning, Inc., Corning, NY) precoated with 2% (w/v) agarose gel (Amresco, Solon, OH) at a density of 3000 cells/well. After incubation for 5 days, uniform and compact spheroids were selected and treated for 7 days with free 5-Fu, DOX or conjugates (equivalent to 10 μg/mL of DOX and 6.2 μg/mL of 5-Fu). The morphology of tumor spheroids was carefully observed by inverted fluorescence microscopy (XD30-RFL, Zhejiang, China).

Cell Cycle Analysis. PC-3 cells were treated with free drugs or conjugates (equivalent to 10 μg/mL of DOX and 6.2 μg/mL of 5-Fu) at 37 °C for 36 h, and then the cells were harvested and washed with PBS. After being fixed with 70% ethanol at −20 °C overnight, the cells

DOI: 10.1021/am509204u
ACS Appl. Mater. Interfaces 2015, 7, 6661−6673

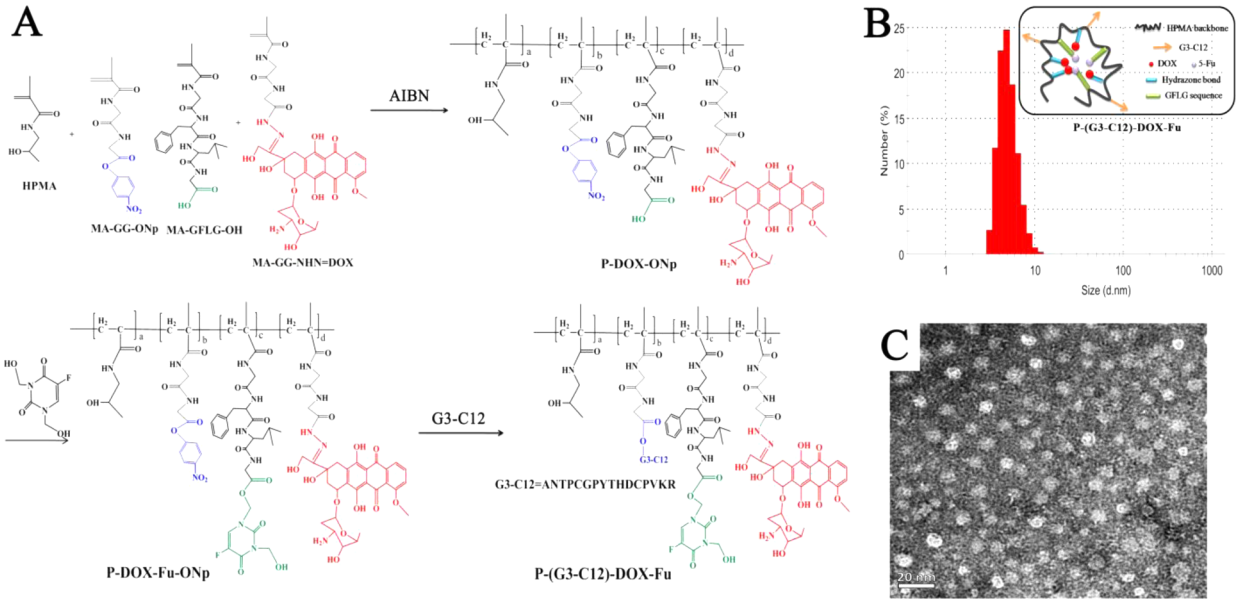

Figure 1. (A) Synthetic pathway and structure of P-(G3-C12)-DOX-Fu. (B) Size distribution of P-(G3-C12)-DOX-Fu by dynamic light scattering. (C) Transmission electron micrographs of P-(G3-C12)-DOX-Fu.

were incubated with RNase A (0.1 mg/mL) for 30 min at 37 °C, and stained with propidium iodide (PI) (0.1 mg/mL) for 30 min in the dark. Cell cycle distribution was analyzed using flow cytometric analysis. The proportions of cells in G0/G1, S, or G2/M phases were depicted as a DNA histogram. Proportions of apoptotic cells, identified based on their hypodiploid DNA content, were estimated by quantifying the SubG1 peak in the cell cycle pattern.

Caspase-3 Activity Assay. The activity of caspase-3 was measured using the Caspase-3 Colorimetric Assay Kit (KeyGEN BioTECH, Nanjing, China) following the manufacturer's protocol. Briefly, PC-3 cells were seeded in 6-well plates and incubated at 37 °C for 24 h with free drugs or conjugates (equivalent to 10 μg/mL of DOX and 6.2 μg/mL of 5-Fu). Cells were then harvested (3−5 × 10^6 cells per sample) and suspended in lysis buffer (150 μL) and incubated in an ice bath for 40 min. The supernatants were collected by centrifugation at 10 000g for 3 min at 4 °C and immediately assayed for total protein using the BCA kit (KeyGEN BioTECH, Nanjing, China). Cell lysates were then placed in 96-well plates containing reaction buffer and caspase-3 substrate, and the plates were incubated for 4 h at 37 °C in the dark. Absorbance at 405 nm was measured using a plate reader (Varioskan Flash, Thermo, Waltham, MA). Caspase-3 activity was expressed as the percentage of control samples, which were treated with fresh culture medium.

Measurement of DNA Damage by Comet Assay. Alkaline single-cell gel electrophoresis (Comet assay) was used to assess DNA damage. PC-3 cells were seeded in 12-well plates, treated at 37 °C for 36 h with free drugs or conjugates (equivalent to 15 μg/mL of DOX and 9.37 μg/mL of 5-Fu), harvested and embedded in 0.6% (w/v) low-melting-temperature agarose on a frosted glass slide precoated with a thin layer of 0.8% (w/v) agarose. The slides were then immersed for 3 h at 4 °C in prechilled lysis solution (2.5 M NaCl, 0.1 M Na_2-EDTA, 10 mM Tris base, pH 10) containing 1% Triton X-100. Finally, DNA released from cells was denatured in alkaline buffer (0.3 M NaCl, 1 mM EDTA) for 30 min at room temperature, and the lysates were subjected to electrophoresis at 25 V and 300 mA for 30 min. The slides were neutralized and stained with SYBR Green dye for 5 min. The comet images were visualized by inverted fluorescence microscopy (CFM 500, Carl Zeiss, Jena, Germany).

Animal Xenograft Model. Male BALB/c nude mice (5−8 weeks old and weighing 20−23 g) were purchased from the Animal Centre of the Institute of West China Medical Center. All animals received care in accordance with guidelines of the animal welfare committee at Sichuan University and the Guide for the Care and Use of Laboratory Animals (NIH publication no. 86-23, revised 1985). To establish human prostate cancer xenografts, PC-3 cells (4 × 10^6 cells/100 μL) were subcutaneously injected into the right flank of the nude mice. When tumors had reached a certain volume, the animals were subjected to various drug treatments as described below.

Internalization of Drugs into Tumor Cells in Vivo. When xenograft tumor volumes reached 300−400 mm^3, mice were divided into four groups (3 animals per group), each of which received tail vein injections of either free DOX, P-DOX, P-DOX-Fu, or P-(G3-C12)-DOX-Fu (equivalent to 8 mg/kg of DOX). After 2 days, mice were sacrificed, and the tumors were removed and fixed overnight with 4% paraformaldehyde. The tumors were then embedded in Tissue Tek OCT compound and frozen at −80 °C. Consecutive frozen sections 6 μm thick were prepared using a Cryostat cryotome (Leica, CM 3050, Germany). Tumor sections were washed with distilled water, stained with DAPI (2 μg/mL) and visualized on a confocal laser scanning microscope (LSM 510 DUE, Carl Zeiss, Jena, Germany).

In Vivo Antitumor Efficacy. When PC-3 xenograft tumor volumes were >100 mm^3, mice were randomly divided into 7 groups (5 animals per group) to receive one of the following treatments: saline, free 5-Fu, free DOX·HCl, P-Fu, P-DOX, P-DOX-Fu, and P-(G3-C12)-DOX-Fu. These treatments were performed on days 0 and 6 by tail injection, the DOX dose was 5 mg/kg and the 5-Fu dose was 3.1 mg/kg. Tumor volumes were measured and calculated every 2 days until day 21 using the formula $V = (LW^2)/2$, where W and L refer to the shortest and longest diameters, respectively. Animal body weight was also monitored throughout the experiment. On day 21, mice were sacrificed, and the major organs, including the heart, liver, spleen, lung, and kidneys, as well as the tumor, were dissected. A portion of tissue was fixed in 10% formalin and embedded in paraffin, and the paraffin-embedded tissues were stained with hematoxylin and eosin (H&E) for histopathological analysis.

Statistical Analysis. Results are presented as mean ± SD. Differences between treatment groups were assessed for statistical significance using Student's t test. Differences were considered significant if the associated p was <0.05 and highly significant if the associated p was <0.01.

RESULTS AND DISCUSSION

Synthesis and Characterization of HPMA Polymer-Drug Conjugates. Drugs can be bound to their polymeric carriers through stimuli-responsive spacers for tumor site

DOI: 10.1021/am509204u
ACS Appl. Mater. Interfaces 2015, 7, 6661−6673

Table 1. Characteristics of Synthesized HPMA Copolymer-Drug Conjugates

conjugate	DOX (wt %)	5-Fu (wt %)	G3-C12 (mol %)	MW (kDa)	PDI	zeta potential (mV)	R_h (nm)
P-Fu		5.73		28.6	1.45	−6.83	4.3
P-DOX	9.47			33.4	1.62	−9.63	4.8
P-DOX-Fu	7.32	4.57		31.7	1.43	−10.4	5.2
P-(G3-C12)-DOX-Fu	7.48	3.88	2.7	36.4	1.57	−12.1	6.8

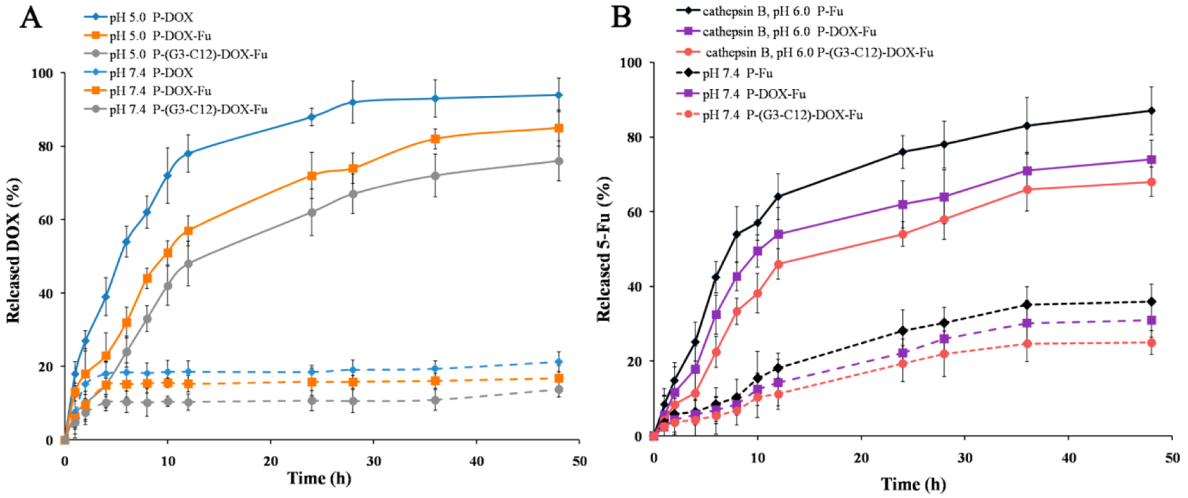

Figure 2. Release profiles of (A) DOX and (B) 5-Fu from HPMA polymer drug conjugates. (A) DOX release from P-DOX, P-DOX-Fu and P-(G3-C12)-DOX-Fu after incubation at 37 °C in phosphate buffer at pH 5.0 or 7.4. (B) Release of 5-Fu from P-Fu, P-DOX-Fu and P-(G3-C12)-DOX-Fu was evaluated by incubating the conjugates at 37 °C in phosphate buffer (0.1 M, pH 7.4) and McIlvaine's buffer (cathepsin B, pH 6.0).

specific drug release.[22] An optimal structure of the GFLG oligopeptide spacer being stable in blood and intracellularly degradable was sorted out for drug attachment.[10] Our previous efforts to conjugate 5-Fu to HPMA copolymer chain have used this enzymatically degradable GFLF oligopeptide.[26,38] This conjugate exhibited 10-fold lower IC_{50} value than free 5-Fu. So GFLG spacer was chosen for 5-Fu attachment in our dual drug-loaded conjugates. In the case of DOX, it has been routinely conjugated to the polymer precursor bearing hydrazide groups via a pH-sensitive hydrazone bond.[34] In comparison with similar conjugates that bound DOX via a GFLG sequence in which the drug loading higher than ∼ 8 wt % results in aggregation in aqueous solutions, this method of DOX attachment via a hydrazone bond allows for much higher loading of the carrier while keeping sufficient solubility of the product.[10] Therefore, we selected hydrazone bond as a linkage between DOX and HPMA copolymer backbone. We hypothesized that the application of different types of spacers for different drugs in a single nanocarrier could guarantee the effective drug release. After endocytosis of drug-loaded nanocarriers into cancer cells, in response to the mildly acidic environment (pH 5−6) of endo/lysosome and a high level of lysosomal proteases, the hydrazone bond and GFLG sequence could be cleaved to impart separate rates of DOX and 5-Fu release, thus allowing agents to act synergistically. In this study, dual drug-loaded HPMA copolymer conjugates decorated with galectin-3-binding peptide G3-C12 [P-(G3-C12)-DOX-Fu] or without the targeting peptide (P-DOX-Fu) were successfully synthesized and characterized for the first time. In parallel, we also synthesized HPMA copolymer conjugates containing only doxorubicin (P-DOX) or 5-fluorouracil (P-Fu) using previous methods; these conjugates served as controls.[34,38] As illustrated in Figure 1A, P-(G3-C12)-DOX-Fu was synthesized by radical precipitation copolymerization of HPMA, MA-GFLG−OH, MA-GG-ONp, and polymerizable drug derivative (MA-GG-NHN=DOX), followed by 5-Fu conjugation and G3-C12 peptide attachment.

Table 1 summarizes key nanocarrier characteristics such as molecular weight, PDI, zeta potential, hydrodynamic radius (R_h), G3-C12 content, and drug loading. Molecular weights of all drug-loaded conjugates fell within the range of 28.6−36.4 kDa with a narrow PDI range <1.62, which were below the renal threshold.[13] The P-(G3-C12)-DOX-Fu formulation showed a G3-C12 content of 2.7 mol %, DOX content of 7.48 wt % and 5-Fu content of 3.88 wt %. The DOX content in our final conjugate P-(G3-C12)-DOX-Fu is 7.48 wt %, which was similar to other HPMA polymer-DOX conjugates.[15] To ensure the solubility of the conjugate, the maximal feed molar ratio of monomer MA-GFLG−OH was 10%, which was used for 5-Fu conjugation. We then adjusted 5-Fu content in P-(G3-C12)-DOX-Fu on this basis. An increase in synergistic cytotoxicity on PC-3 cells was observed as 5-Fu content increased (Figure S1, Supporting Information). Due to the synthetic limitations, no higher drug loading of 5-Fu than 3.88 wt % could be achieved. The spatial structure of DOX in dual drug-loaded HPMA copolymer conjugates resulted in higher steric hindrance for 5-Fu conjugation, which may explain why dual drug-loaded conjugates contained less 5-Fu than P-Fu conjugate did. The slightly negative surface charge of P-(G3-C12)-DOX-Fu (−12.1 mV) would contribute to better blood compatibility.[42] Figure 1B,C shows the R_h obtained by dynamic light scattering (DLS) and transmission electron microscopy (TEM) images of P-(G3-C12)-DOX-Fu coil with an average size less than 10 nm.

In Vitro Drug Release. To maximize the efficacy of combination therapy, we wanted to ensure synergistic effects between the drugs, which requires careful control of the release of each drug.

DOI: 10.1021/am509204u
ACS Appl. Mater. Interfaces 2015, 7, 6661−6673

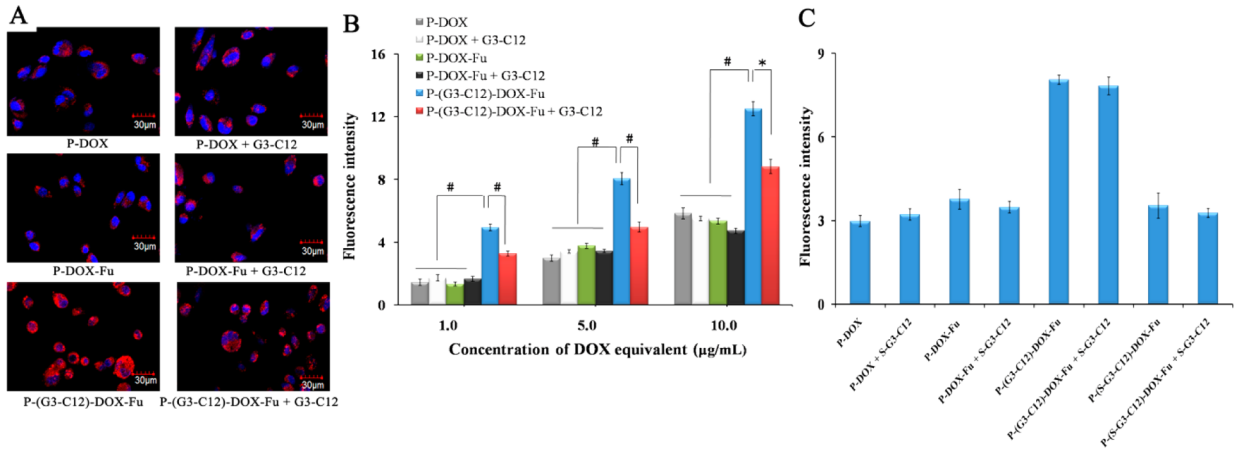

Figure 3. (A) Internalization of various conjugates (equivalent to 5 μg/mL of DOX) by PC-3 human prostate carcinoma cells in the presence or absence of free G3-C12 peptide (200 nM). Cells were incubated with the conjugates for 2 h and analyzed by confocal laser scanning microscopy. Red fluorescence indicates DOX, while blue fluorescence corresponds to DAPI staining of nuclei. (B) Flow cytometric analyses of PC-3 cells after 2 h of incubation with various concentrations of conjugates in the presence or absence of free G3-C12 peptide (200 nM). (C) Flow cytometric analysis of PC-3 cells after 2 h of incubation with various conjugates (equivalent to 5 μg/mL of DOX) in the presence or absence of free scrambled peptide S-G3-C12 (200 nM). Data are presented as the mean ± SD (n = 3, $^{*}p < 0.05$, $^{\#}p < 0.01$).

In one set of experiments, we analyzed DOX release under different pH conditions. As expected, hydrazone spacers of all conjugates were relatively stable at pH 7.4, with less than 21% of DOX released after 48 h (Figure 2A). To simulate the acidic environment of the lysosome, we reduced the pH to 5, which increased release kinetics, such that more than 75% of total drug was released within 48 h from all conjugates. After 48 h at pH 5, P-DOX released 94% of DOX, slightly more than the 83% released from P-DOX-Fu or the 76% released from P-(G3-C12)-DOX-Fu. The lower DOX release from the dual drug-loaded nanocarriers may reflect steric hindrance due to the presence of 5-Fu and G3-C12 peptide. Even so, this lower DOX release rate was still fast enough to provide a high intracellular DOX concentration.

In another set of experiments, we analyzed 5-Fu release in the presence of papain (2.0 μM)[40] or cathepsin B (0.5 μM)[41] to simulate endo/lysosomal conditions. Both proteases can cleave the GFLG linkages between HPMA copolymer chain and the conjugated drug.[40,41] P-Fu showed 5-Fu release of approximately 76% at 24 h and 87% at 48 h in the presence of cathepsin B (Figure 2B). By comparison, P-DOX-Fu had a slightly lower drug release rate: approximately 62% at 24 h and 74% at 48 h. The likely reason could be that the hydrophobic interactions of DOX molecules in the hydrophilic P-DOX-Fu copolymer coil may make the polymer structure more compact, resulting in greater steric hindrance for enzymatic cleavage of the conjugated 5-Fu. P-(G3-C12)-DOX-Fu released 5-Fu in the presence of cathepsin B more slowly compared with P-DOX-Fu, especially initially (32.2 vs 41.5% at 10 h). Approximately 68% of 5-Fu was released from P-(G3-C12)-DOX-Fu within 48 h. To some extent, the attachment of G3-C12 peptide may moderately affect the 5-Fu release. Meanwhile, papain was also used to measure the release of 5-Fu (an enzyme having similar activity as lysosomal cathepsin B).[40] Similar release rates with cathepsin B were obtained (Figure S2, Supporting Information). Control experiments in the absence of lysosomal proteinases showed that spontaneous 5-Fu release was slow and sustained from all conjugates, with approximately 30% of drugs released within 36 h, which may be help to reduce the premature release of 5-Fu extracellularly. These two sets of experiments indicate similar release profiles for both 5-Fu and DOX in an intracellular lysosomal environment. These findings suggest that the targeted codelivery system might allow the two drugs to work synergistically.

Endocytic Uptake. To elucidate the targeting ability of G3-C12-decorated nanovehicle in galectin-3 overexpressed PC-3 cells, confocal microscopy (Figure 3A) and flow cytometry (Figure 3B) were used to assess endocytic uptake of P-DOX, P-DOX-Fu, and P-(G3-C12)-DOX-Fu. As shown in Figure 3A, P-(G3-C12)-DOX-Fu was uptaken by cells to a much greater extent after 2 h than were P-DOX or P-DOX-Fu. For the quantitative study, the fluorescent intensity displayed concentration-dependent behavior (Figure 3B), and no significant difference was observed between P-DOX and P-DOX-Fu at any of the concentrations tested. Uptake was approximately 3-fold higher for G3-C12-modified conjugates than for unmodified conjugates ($p < 0.01$), suggesting the increased affinity of conjugates by G3-C12 peptide decoration. To verify the role of the targeting peptide G3-C12, we performed a competition experiment in which cells were exposed to nanocarriers in the presence of free G3-C12 peptide (Figure 3B). While the free peptide inhibited uptake of P-(G3-C12)-DOX-Fu by 30% ($p < 0.05$), it did not affect uptake of unmodified P-DOX or P-DOX-Fu. This confirms the involvement of galectin-3-mediated endocytosis in uptake of P-(G3-C12)-DOX-Fu.

To exclude nonspecific interaction of G3-C12 peptide and confirm its targeting ability, we synthesized a scrambled version of G3-C12 (S-G3-C12). The scrambled peptide S-G3-C12 possessed the same amino acids as the parent peptide G3-C12 but was randomly changed in primary sequence; and it was conjugated to the dual drug-loaded HPMA copolymer conjugates, namely P-(S-G3-C12)-DOX-Fu. Flow cytometry was used to assess endocytic uptake of P-DOX, P-DOX-Fu, P-(G3-C12)-DOX-Fu, and P-(S-G3-C12)-DOX-Fu (Figure 3C). P-(S-G3-C12)-DOX-Fu exhibited no significant difference of fluorescent intensity compared with P-DOX and P-DOX-Fu, indicating the scrambled peptide S-G3-C12 has no enhancing effect on cell uptake. Moreover, P-(G3-C12)-DOX-Fu has approximately 2.7-fold higher cellular uptake than P-(S-G3-C12)-DOX-Fu. After incubation with various formulations in

DOI: 10.1021/am509204u
ACS Appl. Mater. Interfaces 2015, 7, 6661−6673

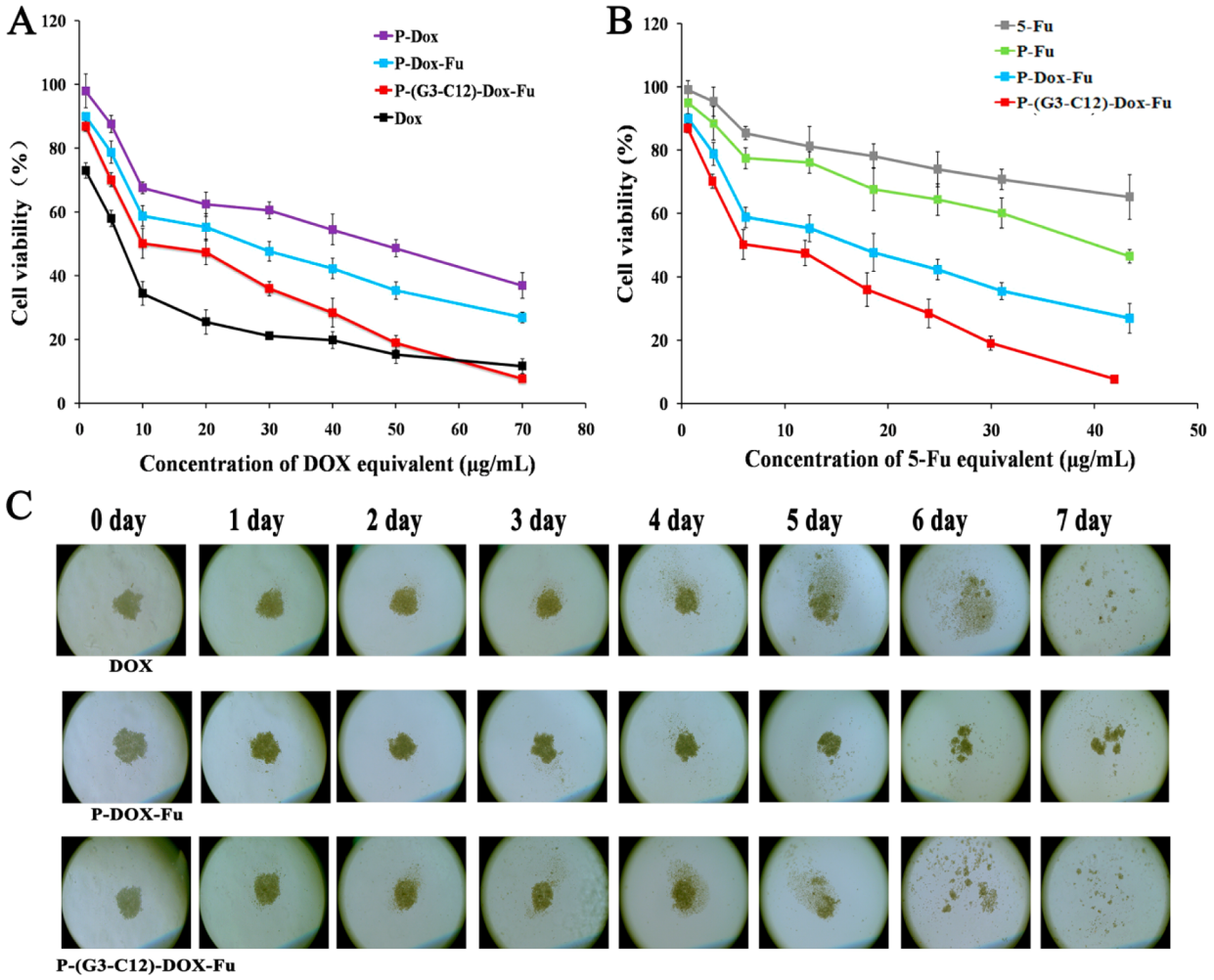

Figure 4. Cell viability of PC-3 cells after 12 h incubation at 37 °C with various concentrations of either (A) free DOX, P-DOX, P-DOX-Fu or P-(G3-C12)-DOX-Fu, or (B) free 5-Fu, P-Fu, P-DOX-Fu, or P-(G3-C12)-DOX-Fu. After incubation with the formulations, the medium was replaced with fresh medium and cells were incubated for another 24 h and finally analyzed by MTT assay. (C) Inhibition of tumor spheroid growth after 7 days of treatment with DOX, P-DOX-Fu or P-(G3-C12)-DOX-Fu (equivalent to 10 μg/mL of DOX and 6.2 μg/mL of 5-Fu).

the presence of free S-G3-C12, it did not affect uptake of all conjugates. These results suggest that the increased affinity of P-(G3-C12)-DOX-Fu was sequence-dependent rather than nonspecific interaction.

In Vitro Cytotoxicity. To investigate whether the enhanced cell uptake by G3-C12-modified dual drug-loaded conjugates could transform into increased anticancer activity, we compared the in vitro antitumor efficacy of free drugs and drug-loaded conjugates in galectin-3 overexpressed PC-3 cells. After 12 h of incubation, the conjugates or drugs were removed, and cells were incubated for another 24 h to allow sufficient intracellular drug release. Finally we assessed cell viability using the MTT assay. The free drugs and all conjugates reduced cell viability in a concentration-dependent manner (Figure 4A,B). P-DOX-Fu was more cytotoxic than 5-Fu or single drug-loaded conjugates over a wide range of drug concentrations. Moreover, P-(G3-C12)-DOX-Fu showed greater cytotoxicity than P-DOX-Fu, and its effects were even comparable to those of free DOX at concentrations equivalent to >50 μg/mL of DOX.

Table 2 summarizes the IC_{50} values of free drugs and drug-loaded conjugates, as well as combination index (CI_{50}) values. The much lower IC_{50} for free DOX than for other formulations makes sense because DOX can easily diffuse across the cell membrane.[43] Conjugation of DOX to the polymeric nanovehicle exhibited greater cytotoxicity than did 5-Fu-loaded ones (IC_{50} = 40.2 ± 2.38 μg/mL of DOX equiv vs IC_{50} = 48.4 ± 3.64 μg/mL of 5-Fu equiv). Co-conjugation of DOX and 5-Fu significantly reduced cell viability (IC_{50} = 21.2 ± 1.28 μg/mL of DOX equiv, $p < 0.01$) relative to single drug-loaded conjugates, demonstrating the synergistic effect of the combination therapy. As expected, cytotoxic effects were significantly stronger with P-(G3-C12)-DOX-Fu (IC_{50} = 11.7 ± 0.87 μg/mL of DOX equiv) than with P-DOX-Fu ($p < 0.01$). This suggests that the G3-C12 peptide substantially boosts the therapeutic potential of the

Table 2. IC_{50} Values and Combination Index (CI_{50}) of Drug Formulations against PC-3 Cells[a]

treatment	IC_{50} Dox (μg/mL)	IC_{50} 5-Fu (μg/mL)	Ci_{50}
DOX	4.88 ± 0.58		
5-Fu		94.37 ± 5.47	
P-DOX	40.2 ± 2.38[bd]		
P-Fu		48.4 ± 3.64[bd]	
P-DOX-Fu	21.2 ± 1.28[d]	14.36 ± 1.34[c]	0.82
P-(G3-C12)-DOX-Fu	11.7 ± 0.87	7.96 ± 0.54	0.46

[a]Data are presented as mean ± SD (n = 5). [b]$p < 0.01$ vs P-DOX-Fu. [c]$p < 0.05$. [d]$p < 0.01$, vs P-(G3-C12)-DOX-Fu).

DOI: 10.1021/am509204u
ACS Appl. Mater. Interfaces 2015, 7, 6661−6673

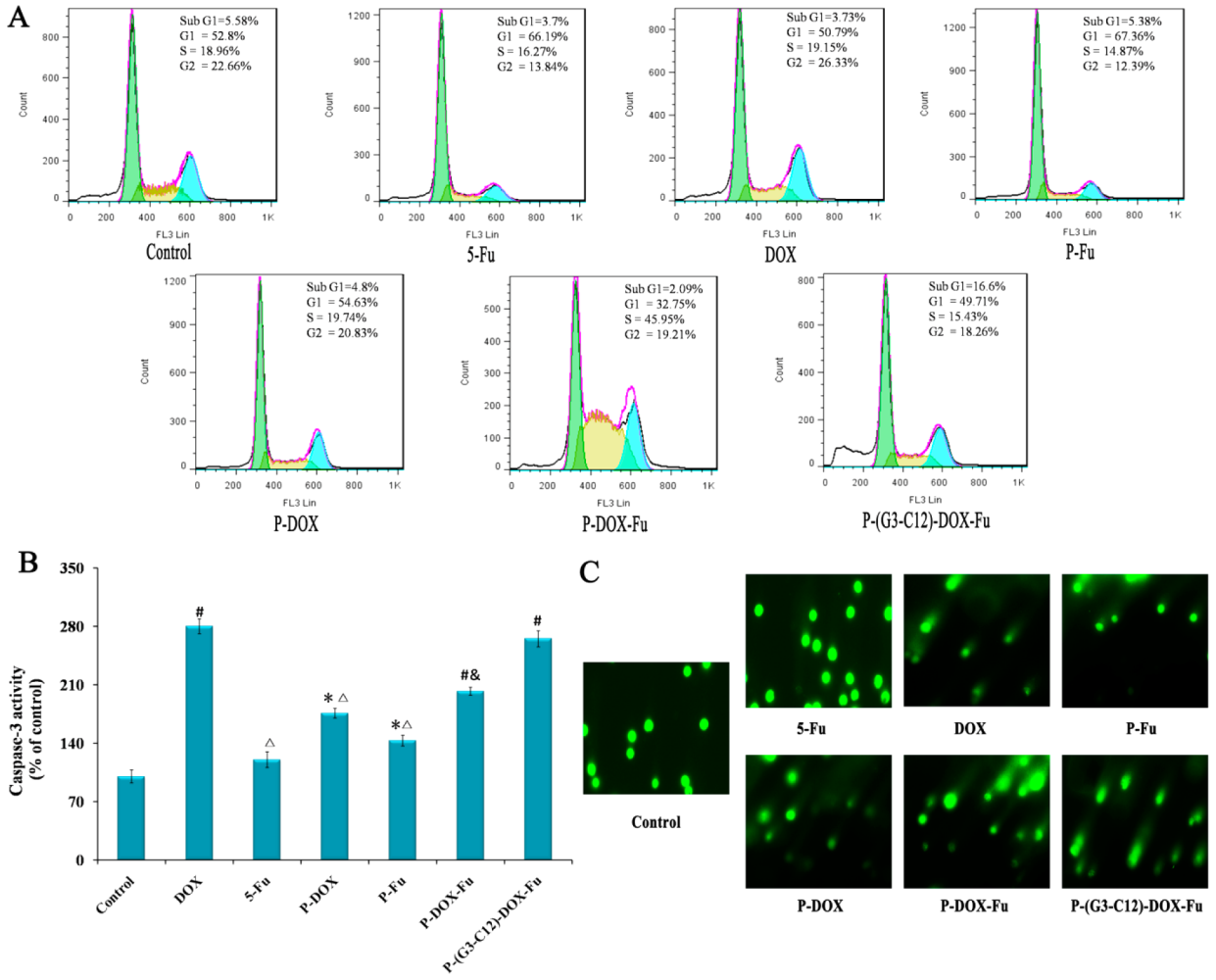

Figure 5. (A) Cell cycle distribution of PC-3 cells after treatment with fresh culture medium (control group), DOX, 5-Fu, P-DOX, P-Fu, P-DOX-Fu, or P-(G3-C12)-DOX-Fu (equivalent to 10 μg/mL of DOX and 6.2 μg/mL of 5-Fu) at 37 °C for 36 h. Cells were then harvested and analyzed by flow cytometry. (B) Caspase-3 activity in PC-3 cells after treatment with various formulations (equivalent to 10 μg/mL of DOX and 6.2 μg/mL of 5-Fu) at 37 °C for 24 h. Enzyme activity was determined using a caspase-3 colorimetric assay. (C) Comet assay to assess DNA damage after treatment with free drugs or conjugates (equivalent to 15 μg/mL of DOX and 9.4 μg/mL of 5-Fu) at 37 °C for 36 h. Single-cell gel electrophoresis assays were performed under alkaline conditions, and DNA was stained with SYBR Green dye. Data are presented as mean ± SD (n = 3, $^{*}p < 0.05$, $^{\#}p < 0.01$ vs control, $^{\&}p < 0.05$, $^{\Delta}p < 0.01$, vs P-(G3-C12)-DOX-Fu).

combination therapy. The combination index (CI) was calculated using the Chou–Talalay isobologram equation.[44] CI values lower than, equal to, or higher than 1 indicate synergism, additivity, or antagonism, respectively. As shown in Table 2, P-DOX-Fu had CI_{50} values below 1 (CI_{50} = 0.82), indicating a synergistic effect. Furthermore, P-(G3-C12)-DOX-Fu exhibited greater synergistic efficiency (CI_{50} = 0.46) than the unmodified conjugates, suggesting that G3-C12-mediated targeting enhanced cytotoxicity.

Three-dimensional tumor spheroids are widely used as an ideal in vitro platform for mimicking solid tumors.[45] In this study, the inhibition of multicellular spheroids growth was evaluated by exposure PC-3 tumor spheroids to different drug formulations for 7 days. Spheroids exposed to fresh culture medium continued to grow and eventually became more compact (Figure S3, Supporting Information) due to cell proliferation of outer layers in the spheroids. On the contrary, the various drug formulations inhibited spheroids growth to the same relative extent as observed in the MTT assay. Treatment of P-DOX-Fu significantly inhibited spheroid growth for 7 days and spheroids finally disintegrating on day 7 as compared to free 5-Fu, P-DOX or P-Fu (Figure 4C and Figure S3, Supporting Information), suggesting a synergistic therapeutic effect from dual drug-loaded nanocarriers. The targeted P-(G3-C12)-DOX-Fu showed the greatest spheroids growth inhibition. On day 4, the spheroids showed loosening and breaking up from the outer perimeter, and they totally collapsed on day 6 (Figure 4C). This result indicates that G3-C12 decoration of polymer-drug conjugates can more efficiently inhibit the growth of PC-3 tumor spheroid.

Induction of Synergistic Genotoxicity. The effectiveness of many anticancer drugs depends on their ability to damage DNA, generating lesions that ultimately induce cell death.[46] With the aim of investigating whether the combination of DOX and 5-Fu will produce synergistic genotoxicity, cell cycle distribution, caspase-3 activity and DNA damage efficacy in PC-3 cell exposed to different drug formulations were studied.

First, DNA flow cytometric analysis was performed to examine how the drugs affected cell cycle distribution. Cells with irreversible DNA damage should undergo apoptosis, appearing as an increase in the proportion of cells in the SubG1 phase.[47] Treating cells with free DOX, free 5-Fu, P-DOX, or P-

DOI: 10.1021/am509204u
ACS Appl. Mater. Interfaces 2015, 7, 6661–6673

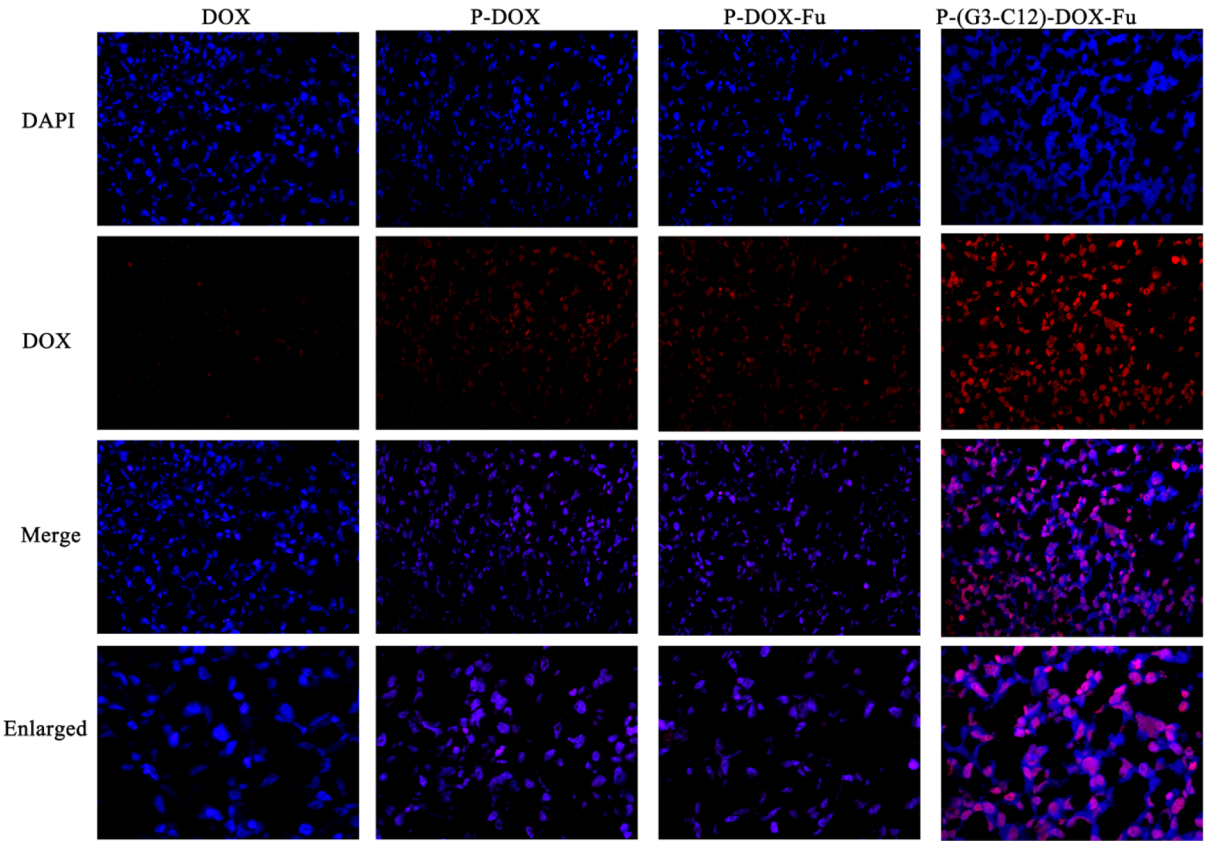

Figure 6. Confocal laser scanning micrographs of PC-3 tumors sections dissected 48 h after intravenous injection of free DOX, P-DOX, P-DOX-Fu, or P-(G3-C12)-DOX-Fu (equivalent to 8 mg/kg DOX). Red fluorescence corresponds to DOX; blue fluorescence signal derived from nuclei stained by DAPI.

Fu alone (equivalent to 10 μg/mL of DOX and 6.2 μg/mL of 5-Fu) for 36 h led to similar cell cycle distributions with treating cells with fresh culture medium (Figure 5A); in no case did the proportion of cells in SubG1 exceed 6%. In contrast, treating cells with P-DOX-Fu significantly altered the cell cycle distribution, reducing the proportion of cells in G1 phase (32.75%) and increasing the proportion arrested in S phase (45.95%). This suggests that simultaneous release of DOX and 5-Fu causes S phase arrest, which may explain the cytotoxicity of P-DOX-Fu. Most notably, the exposure of PC-3 cells to P-(G3-C12)-DOX-Fu significantly increased the proportion of apoptotic cells to 16.6% in SubG1 compared to 5.58% in control group.

Caspases form a family of cysteine proteases that cleave various cellular substrates to drive apoptosis.[48] To explore whether the activation of caspase (caspase-3) is involved in cell death induced by dual drug-loaded conjugates, we used a colorimetric assay to analyze the activation of caspase-3 in PC-3 cells exposed to different drug formulations for 24 h (equivalent to 10 μg/mL of DOX and 6.2 μg/mL of 5-Fu). All drug formulations evoked activation of caspase-3, albeit to different extents (Figure 5B). Treating cells with P-DOX-Fu led to 1.15-fold higher caspase-3 activity than treating them with P-DOX, 1.41-fold higher than with P-Fu and 1.68-fold higher than with 5-Fu. In addition, P-(G3-C12)-DOX-Fu triggered 1.32-fold greater caspase-3 activation than P-DOX-Fu, suggesting that G3-C12-decorated conjugates induced apoptotic cell death primarily via caspase-dependent pathways. These results further support the superiority of combination therapy. P-(G3-C12)-DOX-Fu activated caspase-3 (2.65-fold relative to control) to a similar extent as free DOX (2.8-fold). This may reflect the controlled drug release from P-(G3-C12)-DOX-Fu as well as the fact that free DOX could quickly display its effects after entering cells via passive diffusion.

Because caspase-3 is the primary activator of apoptotic internucleosomal DNA fragmentation,[49] we verified and extended the above activation assays using the comet assay. We treated PC-3 cells with different drug formulations for 36 h (equivalent to 15 μg/mL of DOX and 9.4 μg/mL of 5-Fu) and measured the length of the comet tail, which correlates with the extent of DNA damage.[50] A small number of DNA fragments was observed in cells treated with P-DOX or P-Fu, but they were barely detectable in cells treated with 5-Fu (Figure 5C). Significantly more DNA fragments occurred in cells treated with P-DOX-Fu, showing that codelivery of DOX and 5-Fu markedly potentiated DNA damage. Even more pronounced DNA damage was observed with P-(G3-C12)-DOX-Fu, which was accompanied by a parallel increase in caspase-3 activation (Figure 5B).

Taken together, these results show that combining DOX and 5-Fu into a single HPMA polymer potentiates cell cycle arrest, caspase-3 activation and DNA damage, constituting synergistic genotoxicity. Furthermore, reinforcing the affinity of the conjugates to tumor cells by attaching the G3-C12 peptide maximizes cell genotoxicity.

Intracellular Drug Delivery in Tumors. Efficient cancer cell uptake of chemotherapeutics is essential to achieve effective chemotherapy responses.[51] In previous work, we showed that decorating HPMA polymers with G3-C12 peptide improves accumulation of the nanocarriers in xenograft tumors in

DOI: 10.1021/am509204u
ACS Appl. Mater. Interfaces 2015, 7, 6661−6673

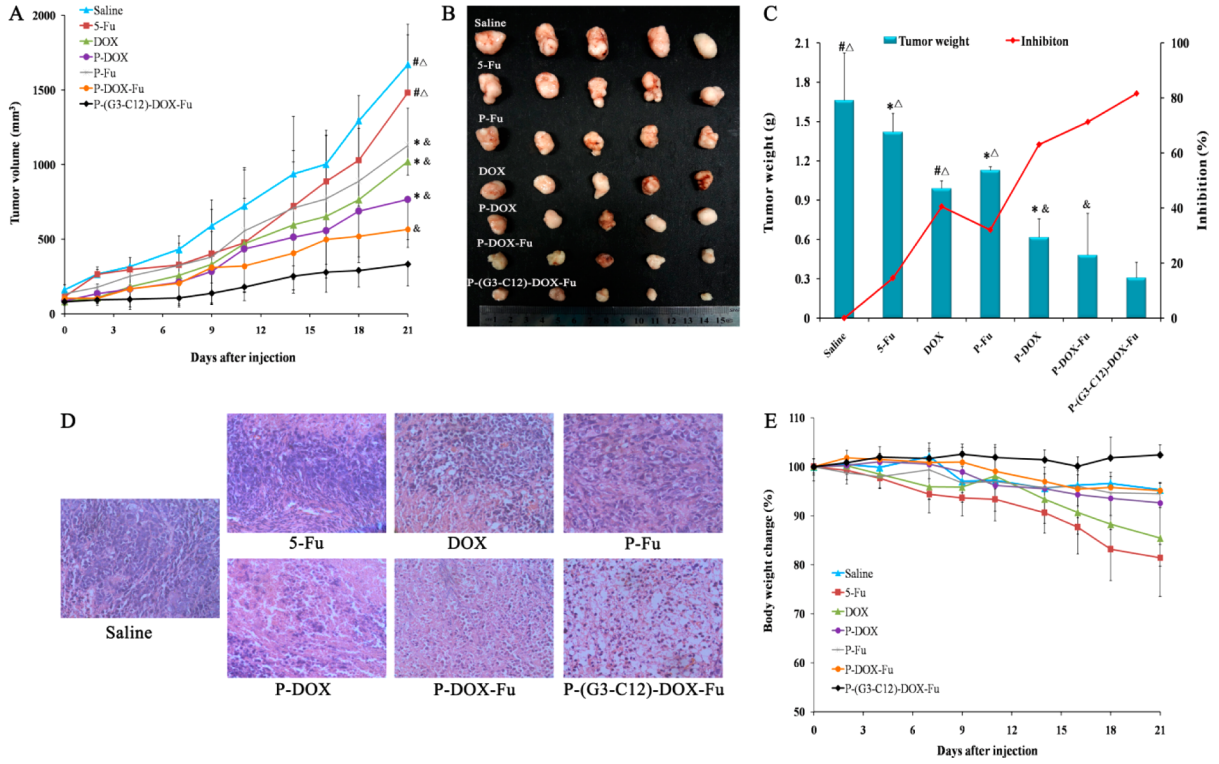

Figure 7. In vivo anticancer efficacy of drug formulations. (A) Tumor growth inhibition effects of different formulations on PC-3 xenograft-bearing mice. On days 0 and 6, mice were intravenously administered saline, free 5-Fu, DOX·HCl, P-Fu, P-DOX, P-DOX-Fu, and P-(G3-C12)-DOX-Fu (DOX dose at 5 mg/kg, 5-Fu at 3.1 mg/kg). On day 21, mice were sacrificed, (B) PC-3 tumors were photographed, and (C) isolated tumors were weighed. (D) Histological examination of tumors using hematoxylin and eosin (H&E) staining after treatment. (E) Body weight changes in mice bearing PC-3 tumors after treatment with different formulations. Data are presented as mean ± SD ($n = 5$, $^{*}p < 0.05$, $^{\#}p < 0.01$ vs P-DOX-Fu, $^{\&}p < 0.05$, $^{\Delta}p < 0.01$, vs P-(G3-C12)-DOX-Fu).

mice.[26,27] To extend these results by showing directly that the peptide enhances intracellular delivery of P-(G3-C12)-DOX-Fu in tumors, we injected mice bearing xenograft PC-3 tumors with free DOX, P-DOX, P-DOX-Fu, or P-(G3-C12)-DOX-Fu and dissected the tumor tissue 48 h later (Figure 6). We used confocal microscopy to examine red fluorescence due to DOX and blue fluorescence due to DAPI staining of nuclei. Mice treated with P-(G3-C12)-DOX-Fu showed higher red fluorescence intensity in tumor than mice treated with other formulations; the fluorescence was widely distributed throughout the tumor tissue, even a great amount of red signals was seen to arrive at nucleus. Much less but still abundant red fluorescence was visible in tumors from animals treated with the unmodified conjugates P-DOX or P-DOX-Fu, reflecting the EPR effect. In contrast, red fluorescence was barely detectable in tumors treated with free DOX alone. These results suggest that, based on the EPR effect, decorating dual drug-loaded polymeric nanovehicles with G3-C12 peptide allows them to enter tumor cells more efficiently, which is consistent with the observations of in vitro cell uptake experiments.

In Vivo Antitumor Activity. Encouraged by these observations, we investigated the antitumor therapeutic efficacy of the various drug formulations in mice bearing PC-3 xenograft tumors. Mice were treated with saline or different drug formulations on days 0 and 6; the DOX dose was 5 mg/kg and the 5-Fu dose was 3.1 mg/kg. While tumors grew rapidly in mice injected with saline, all the drug formulations showed efficacy in tumor regression to different extents (Figure 7A). Though better inhibition of tumor growth was achieved by single drug-loaded conjugates (P-DOX and P-Fu) as compared to the corresponding free drugs, codelivery of DOX and 5-Fu (P-DOX-Fu) showed more efficient suppression on tumor growth ($p < 0.05$). Moreover, in comparison with nontargeted P-DOX-Fu, the targeted P-(G3-C12)-DOX-Fu exhibited the most potent anticancer efficacy. Tumor volume in mice treated with P-(G3-C12)-DOX-Fu at the end of the trial was only 18.8% of the tumor volume in saline-injected mice, 2.31-fold and 1.7-fold smaller than that the volume in mice treated with P-DOX and P-DOX-Fu, respectively. Tumor samples were collected at the end of the experiment and weighted (Figure 7B,C). Tumors from mice that received any of the chemotherapeutic agents weighed significantly less than those from saline-treated group. Therapeutic activity was highest with P-(G3-C12)-DOX-Fu treated group (tumor inhibition of 81.6%), next higher with P-DOX-Fu (71.2%), followed by P-DOX (63%), then free DOX (40.5%) and P-Fu (32.0%), and finally 5-Fu (14.6%).

To examine the in vivo effects of various drug formulations at the cellular level, tumors were dissected from mice on day 21 for histological analysis using hematoxylin and eosin (H&E) staining. Normal tumor cells had large nuclei with a spherical or spindle shape and abundant chromatin. Necrotic cells, in contrast, lacked a definite morphology, and the chromatin became darker and shrunken.[52] In the saline-treated control mice, tumor cells had large nuclei and abundant chromatin, indicating vigorous tumor growth (Figure 7D). The various drug formulations caused varying degrees of tumor necrosis, consistent with the results of in vivo antitumor efficacy. The unmodified dual drug-loaded conjugates (P-DOX-Fu) created a larger necrosis area than monotherapy. Treating animals with

DOI: 10.1021/am509204u
ACS Appl. Mater. Interfaces 2015, 7, 6661−6673

P-(G3-C12)-DOX-Fu led to the most severe necrosis in the tumor, including evident pyknosis of nuclei and condensation of the cytoplasm. The superior antitumor effect of P-(G3-C12)-DOX-Fu might be ascribed to the EPR effect of HPMA polymers, the simultaneous delivery of sufficient amounts of two drugs to the tumor site, elevated cell uptake into the tumor tissue as a result of ligand conjugation, and the synergistic effect of DOX and 5-Fu on tumor regression.

Considering that simultaneous intravenous injection of DOX and 5-Fu may cause systemic toxicity,[53,54] it is necessary to evaluate the safety of the dual drug-loaded conjugates. As a preliminary measure of in vivo safety and tolerance, we examined changes in body weight (Figure 7E). Treatment with P-DOX-Fu or P-(G3-C12)-DOX-Fu did not lead to any significant changes in body weight change during the study period. This indicates the excellent tolerability of these drug regimens. On the contrary, mice treated with free DOX or 5-Fu lost 18.5 or 14.6% of body weight, respectively, during the course of study, indicating serious systemic toxicity. To assess chronic toxicity levels of various drug formulations, the hearts, livers, spleens, lungs, and kidneys were dissected on day 21 and stained with H&E for histological analysis. Obvious accumulation of neutrophils was observed in the hearts of mice treated with free DOX but not in the hearts from other treatment groups, indicating that free DOX possessed evident cardiac toxicity in line with other studies (Figure S4, Supporting Information).[7] In contrast, we failed to detect any acute pathological changes in mice treated with 5-Fu, P-Fu, or DOX-loaded HPMA polymer conjugates, demonstrating that conjugation of DOX to HPMA polymers can reduce the cardiac toxicity of free DOX. This may be reflect different pharmacokinetics between free DOX and DOX conjugated to HPMA polymers.[22] Moreover, the histological examination showed that the drug-loaded conjugates did not cause obvious changes in other major organs (liver, spleen, lung, or kidney); these tissues were very similar to those from mice treated with saline. Together, these data clearly show the low toxicity and high tolerability of HPMA copolymer-based combination therapy in vivo.

CONCLUSIONS

In this study, we have described the synthesis and characterization of G3-C12-modified HPMA copolymer conjugates for codelivery of DOX and 5-Fu [P-(G3-C12)-DOX-Fu]. DOX was covalently conjugated to the nanocarrier using a pH-sensitive hydrazone bond, and 5-Fu was conjugated using an enzymatically degradable oligopeptide GFLG sequence. G3-C12 peptide was attached to the conjugates to facilitate intracellular uptake of both drugs. In galectin-3 overexpressed PC-3 human prostate carcinoma cells, P-(G3-C12)-DOX-Fu showed greater cytotoxicity than other drug conjugates and similar cytotoxicity as free DOX at high concentration. This higher cytotoxicity was due to more efficient uptake by cells and to synergistic genotoxicity involving cell cycle arrest, caspase-3 activation and DNA damage. In vivo experiments showed that P-(G3-C12)-DOX-Fu caused significantly stronger tumor growth inhibition (81.6%) than did nontargeted P-DOX-Fu (71.2%), P-DOX (63%), DOX·HCl (40.5%), P-Fu (32.0%), or 5-Fu (14.6%). This suggests that codelivery of DOX and 5-Fu in G3-C12-modified HPMA polymer conjugates would be promising for prostate cancer treatment due to high therapeutic efficacy and low systemic toxicity.

ASSOCIATED CONTENT

Supporting Information

Cytotoxicity of different C3-C12 modified dual drug-loaded conjugates; release of 5-Fu from conjugates in the presence of papain; inhibition of tumor spheroid growth after treatment with 5-Fu, P-Fu, or P-DOX for 7 days; histological examination of major organs after hematoxylin and eosin (H&E) staining. This material is available free of charge via the Internet at http://pubs.acs.org.

AUTHOR INFORMATION

Corresponding Author

*E-mail: huangyuan0@163.com. Tel.: +86-28-85501617. Fax: +86-28-85501617.

Author Contributions

†These authors contributed equally to this work.

Notes

The authors declare no competing financial interest.

ACKNOWLEDGMENTS

This research was supported by the National Natural Science Foundation of China (81473167) and the Doctoral Fund of Ministry of Education of China (2013018111001).

REFERENCES

(1) Ascierto, P. A.; Marincola, F. M. Combination Therapy: The Next Opportunity and Challenge of Medicine. *J. Transl. Med.* **2011**, *9*, 115.

(2) Mehta, R. S.; Barlow, W. E.; Albain, K. S.; Vandenberg, T. A.; Dakhil, S. R.; Tirumali, N. R.; Lew, D. L.; Hayes, D. F.; Gralow, J. R.; Livingston, R. B.; Hortobagyi, G. N. Combination Anastrozole and Fulvestrant in Metastatic Breast Cancer. *N. Engl. J. Med.* **2012**, *367*, 435−444.

(3) Joensuu, H.; Holli, K.; Heikkinen, M.; Suonio, E.; Aro, A. R.; Hietanen, P.; Huovinen, R. Combination Chemotherapy versus Single-Agent Therapy as First- and Second-Line Treatment in Metastatic Breast Cancer: a Prospective Randomized Trial. *J. Clin. Oncol.* **1998**, *16*, 3720−3730.

(4) Peer, D.; Karp, J. M.; Hong, S.; Farokhzad, O. C.; Margalit, R.; Langer, R. Nanocarriers as an Emerging Platform for Cancer Therapy. *Nat. Nanotechnol.* **2007**, *2*, 751−760.

(5) Zhang, Y. F.; Wang, J. C.; Bian, D. Y.; Zhang, X.; Zhang, Q. Targeted Delivery of RGD-Modified Liposomes Encapsulating both Combretastatin A-4 and Doxorubicin for Tumor Therapy: In Vitro and in Vivo Studies. *Eur. J. Pharm. Biopharm.* **2010**, *74*, 467−473.

(6) Wang, H.; Zhao, Y.; Wu, Y.; Hu, Y. L.; Nan, K.; Nie, G.; Chen, H. Enhanced Anti-Tumor Efficacy by Co-Delivery of Doxorubicin and Paclitaxel with Amphiphilic Methoxy PEG-PLGA Copolymer Nanoparticles. *Biomaterials* **2011**, *32*, 8281−8290.

(7) Duan, X.; Xiao, J.; Yin, Q.; Zhang, Z.; Yu, H.; Mao, S.; Li, Y. Smart pH-Sensitive and Temporal-Controlled Polymeric Micelles for Effective Combination Therapy of Doxorubicin and Disulfiram. *ACS Nano* **2013**, *7*, 5858−5869.

(8) Li, Z.-Y.; Liu, Y.; Wang, X.-Q.; Liu, L.-H.; Hu, J.-J.; Luo, G.-F.; Chen, W.-H.; Rong, L.; Zhang, X.-Z. One-Pot Construction of Functional Mesoporous Silica Nanoparticles for the Tumor-Acidity-Activated Synergistic Chemotherapy of Glioblastoma. *ACS Appl. Mater. Interfaces* **2013**, *5*, 7995−8001.

(9) Wang, H.; Li, F.; Du, C.; Wang, H.; Mahato, R. I.; Huang, Y. Doxorubicin and Lapatinib Combination Nanomedicine for Treating Resistant Breast Cancer. *Mol. Pharmaceutics* **2014**, *11*, 2600−2611.

(10) Ulbrich, K.; Šubr, V. Structural and Chemical Aspects of HPMA Copolymers as Drug Carriers. *Adv. Drug Delivery Rev.* **2010**, *62*, 150−166.

(11) Larson, N.; Ghandehari, H. Polymeric Conjugates for Drug Delivery. *Chem. Mater.* **2012**, *24*, 840−853.

DOI: 10.1021/am509204u
ACS Appl. Mater. Interfaces 2015, 7, 6661−6673

(12) Yang, J.; Kopeček, J. Macromolecular Therapeutics. *J. Controlled Release* **2014**, *190*, 288−303.
(13) Kopeček, J. Polymer-Drug Conjugates: Origins, Progress to Date and Future Directions. *Adv. Drug Delivery Rev.* **2013**, *65*, 49−59.
(14) Krakovicova, H.; Etrych, T.; Ulbrich, K. HPMA-Based Polymer Conjugates with Drug Combination. *Eur. J. Pharm. Sci.* **2009**, *37*, 405−412.
(15) Kostková, H.; Etrych, T.; Říhová, B.; Ulbrich, K. Synergistic Effect of HPMA Copolymer-Bound Doxorubicin and Dexamethasone in Vivo on Mouse Lymphomas. *J. Bioact. Compat. Polym.* **2011**, *26*, 270−286.
(16) Lammers, T.; Subr, V.; Ulbrich, K.; Peschke, P.; Huber, P. E.; Hennink, W. E.; Storm, G. Simultaneous Delivery of Doxorubicin and Gemcitabine to Tumors in Vivo Using Prototypic Polymeric Drug Carriers. *Biomaterials* **2009**, *30*, 3466−3475.
(17) Zhou, Y.; Yang, J.; Rhim, J. S.; Kopeček, J. HPMA Copolymer-Based Combination Therapy Toxic to Both Prostate Cancer Stem/Progenitor Cells and Differentiated Cells Induces Durable Anti-Tumor Effects. *J. Controlled Release* **2013**, *172*, 946−953.
(18) Kostkova, H.; Etrych, T.; Rihova, B.; Kostka, L.; Starovoytova, L.; Kovar, M.; Ulbrich, K. HPMA Copolymer Conjugates of DOX and Mitomycin C for Combination Therapy: Physicochemical Characterization, Cytotoxic Effects, Combination Index Analysis, and Anti-Tumor Efficacy. *Macromol. Biosci.* **2013**, *13*, 1648−1660.
(19) Karhadkar, S. S.; Bova, G. S.; Abdallah, N.; Dhara, S.; Gardner, D.; Maitra, A.; Isaacs, J. T.; Berman, D. M.; Beachy, P. A. Hedgehog Signalling in Prostate Regeneration, Neoplasia and Metastasis. *Nature* **2004**, *431*, 707−712.
(20) Greco, F.; Vicent, M. J. Combination Therapy: Opportunities and Challenges for Polymer-Drug Conjugates as Anticancer Nanomedicines. *Adv. Drug Delivery Rev.* **2009**, *61*, 1203−1213.
(21) Lammers, T. Improving the Efficacy of Combined Modality Anticancer Therapy Using HPMA Copolymer-Based Nanomedicine Formulations. *Adv. Drug Delivery Rev.* **2010**, *62*, 203−230.
(22) Kopeček, J.; Kopečková, P. HPMA Copolymers: Origins, Early Developments, Present, and Future. *Adv. Drug Delivery Rev.* **2010**, *62*, 122−149.
(23) Lammers, T.; Subr, V.; Ulbrich, K.; Hennink, W. E.; Storm, G.; Kiessling, F. Polymeric Nanomedicines for Image-Guided Drug Delivery and Tumor-Targeted Combination Therapy. *Nano Today* **2010**, *5*, 197−212.
(24) Pike, D. B.; Ghandehari, H. HPMA Copolymer−Cyclic RGD Conjugates for Tumor Targeting. *Adv. Drug Delivery Rev.* **2010**, *62*, 167−183.
(25) Boscher, C.; Dennis, J. W.; Nabi, I. R. Glycosylation, Galectins, and Cellular Signaling. *Curr. Opin. Cell Biol.* **2011**, *23*, 383−392.
(26) Yang, Y.; Zhou, Z.; He, S.; Fan, T.; Jin, Y.; Zhu, X.; Chen, C.; Zhang, Z.-r.; Huang, Y. Treatment of Prostate Carcinoma with (Galectin-3)-Targeted HPMA Copolymer-(G3-C12)-5-Fluorouracil Conjugates. *Biomaterials* **2012**, *33*, 2260−2271.
(27) Yang, Y.; Li, L.; Zhou, Z.; Yang, Q.; Liu, C.; Huang, Y. Targeting Prostate Carcinoma by G3-C12 Peptide Conjugated *N*-(2-Hydroxypropyl)methacrylamide Copolymers. *Mol. Pharmaceutics* **2014**, *11*, 3251−3260.
(28) Binaschi, M.; Zunino, F.; Capranico, G. Mechanism of Action of DNA Topoisomerase Inhibitors. *Stem Cells* **1995**, *13*, 369−379.
(29) Vincent, J.; Mignot, G.; Chalmin, F.; Ladoire, S.; Bruchard, M.; Chevriaux, A.; Martin, F.; Apetoh, L.; Rebe, C.; Ghiringhelli, F. 5-Fluorouracil Selectively Kills Tumor-Associated Myeloid-Derived Suppressor Cells Resulting in Enhanced T Cell-Dependent Antitumor Immunity. *Cancer Res.* **2010**, *70*, 3052−3061.
(30) Jassem, J.; Pienkowski, T.; Pluzanska, A.; Jelic, S.; Gorbunova, V.; Mrsic-Krmpotic, Z.; Berzins, J.; Nagykalnai, T.; Wigler, N.; Renard, J.; Munier, S.; Weil, C.; Central and Eastern Europe and Israel Pacitaxel Breast Cancer Study Group. Doxorubicin and Paclitaxel versus Fluorouracil, Doxorubicin, and Cyclophosphamide as First-Line Therapy for Women with Metastatic Breast Cancer: Final Results of a Randomized Phase III Multicenter Trial. *J. Clin. Oncol.* **2001**, *19*, 1707−1715.
(31) Smith, F. P.; Hoth, D. F.; Levin, B.; Karlin, D. A.; MacDonald, J. S.; Woolley, P. V., III; Schein, P. S. 5-Fluorouracil, Adriamycin, and Mitomycin-C (FAM) Chemotherapy for Advanced Adenocarcinoma of the Pancreas. *Cancer* **1980**, *46*, 2014−2018.
(32) Ding, X.; Liu, Y.; Li, J.; Luo, Z.; Hu, Y.; Zhang, B.; Liu, J.; Zhou, J.; Cai, K. Hydrazone-Bearing PMMA-Functionalized Magnetic Nanocubes as pH-Responsive Drug Carriers for Remotely Targeted Cancer Therapy in Vitro and in Vivo. *ACS Appl. Mater. Interfaces* **2014**, *6*, 7395−7407.
(33) Ulbrich, K.; Subr, V.; Strohalm, J.; Plocova, D.; Jelinkova, M.; Rihova, B. Polymeric Drugs Based on Conjugates of Synthetic and Natural Macromolecules. I. Synthesis and Physico-Chemical Characterisation. *J. Controlled Release* **2000**, *64*, 63−79.
(34) Etrych, T.; Mrkvan, T.; Chytil, P.; Koňák, Č.; Říhová, B.; Ulbrich, K. *N*-(2-Hydroxypropyl) Methacrylamide-Based Polymer Conjugates with pH-Controlled Activation of Doxorubicin. I. New Synthesis, Physicochemical Characterization and Preliminary Biological Evaluation. *J. Appl. Polym. Sci.* **2008**, *109*, 3050−3061.
(35) Rejmanová, P.; Labský, J.; Kopeček, J. Aminolyses of Monomeric and Polymeric 4-Nitrophenyl Esters of *N*-Methacryloylamino Acids. *Macromol. Chem. Phys.* **1977**, *178*, 2159−2168.
(36) Yuan, F.; Chen, F.; Xiang, Q. Y.; Qin, X.; Zhang, Z. R.; Huang, Y. Synthesis and Characterization of HPMA Copolymer-5-FU Conjugates. *Chin. Chem. Lett.* **2008**, *19*, 137−140.
(37) Rathi, R. C.; Kopečková, P.; Říhová, B.; Kopeček, J. *N*-(2-hydroxypropyl) Methacrylamide Copolymers Containing Pendant Saccharide Moieties: Synthesis and Bioadhesive Properties. *J. Polym. Sci., Part A: Polym. Chem.* **1991**, *29*, 1895−1902.
(38) Yuan, F.; Qin, X.; Zhou, D.; Xiang, Q. Y.; Wang, M. T.; Zhang, Z. R.; Huang, Y. In Vitro Cytotoxicity, in Vivo Biodistribution and Antitumor Activity of HPMA Copolymer-5-Fluorouracil Conjugates. *Eur. J. Pharm. Biopharm.* **2008**, *70*, 770−776.
(39) Etrych, T.; Jelínková, M.; Říhová, B.; Ulbrich, K. New HPMA Copolymers Containing Doxorubicin Bound via pH-Sensitive Linkage: Synthesis and Preliminary in Vitro and in Vivo Biological Properties. *J. Controlled Release* **2001**, *73*, 89−102.
(40) Zhang, R.; Luo, K.; Yang, J.; Sima, M.; Sun, Y.; Janát-Amsbury, M. M.; Kopeček, J. Synthesis and Evaluation of a Backbone Biodegradable Multiblock HPMA Copolymer Nanocarrier for the Systemic Delivery of Paclitaxel. *J. Controlled Release* **2013**, *166*, 66−74.
(41) Etrych, T.; Strohalm, J.; Chytil, P.; Černoch, P.; Starovoytova, L.; Pechar, M.; Ulbrich, K. Biodegradable Star HPMA Polymer Conjugates of Doxorubicin for Passive Tumor Targeting. *Eur. J. Pharm. Sci.* **2011**, *42*, 527−539.
(42) Du, J. Z.; Du, X. J.; Mao, C. Q.; Wang, J. Tailor-Made Dual pH-Sensitive Polymer-Doxorubicin Nanoparticles for Efficient Anticancer Drug Delivery. *J. Am. Chem. Soc.* **2011**, *133*, 17560−17563.
(43) Zhang, C.; Pan, D.; Luo, K.; She, W.; Guo, C.; Yang, Y.; Gu, Z. Peptide Dendrimer-Doxorubicin Conjugate-Based Nanoparticles as an Enzyme-Responsive Drug Delivery System for Cancer Therapy. *Adv. Healthcare Mater.* **2014**, *3*, 1299−1308.
(44) Chou, T. C. Drug Combination Studies and Their Synergy Quantification Using the Chou−Talalay Method. *Cancer Res.* **2010**, *70*, 440−446.
(45) Wang, X.; Zhen, X.; Wang, J.; Zhang, J.; Wu, W.; Jiang, X. Doxorubicin Delivery to 3D Multicellular Spheroids and Tumors Based on Boronic Acid-Rich Chitosan Nanoparticles. *Biomaterials* **2013**, *34*, 4667−4679.
(46) Helleday, T.; Petermann, E.; Lundin, C.; Hodgson, B.; Sharma, R. A. DNA Repair Pathways as Targets for Cancer Therapy. *Nat. Rev. Cancer* **2008**, *8*, 193−204.
(47) Ishikawa, K.; Ishii, H.; Saito, T. DNA Damage-Dependent Cell Cycle Checkpoints and Genomic Stability. *DNA Cell Biol.* **2006**, *25*, 406−411.
(48) Fulda, S. Targeting Apoptosis for Anticancer Therapy. *Semin. Cancer Biol.* **2015**, *31*, 84−88.
(49) McIlroy, D.; Sakahira, H.; Talanian, R. V.; Nagata, S. Involvement of Caspase 3-Activated DNase in Internucleosomal

DOI: 10.1021/am509204u
ACS Appl. Mater. Interfaces 2015, 7, 6661−6673

DNA Cleavage Induced by Diverse Apoptotic Stimuli. *Oncogene* **1999**, *18*, 4401−4408.
(50) AshaRani, P. V.; Low Kah Mun, G.; Hande, M. P.; Valiyaveettil, S. Cytotoxicity and Genotoxicity of Silver Nanoparticles in Human Cells. *ACS Nano* **2009**, *3*, 279−290.
(51) Lammers, T.; Kiessling, F.; Hennink, W. E.; Storm, G. Drug Targeting to Tumors: Principles, Pitfalls and (Pre-) Clinical Progress. *J. Controlled Release* **2012**, *161*, 175−187.
(52) Lv, S.; Tang, Z.; Li, M.; Lin, J.; Song, W.; Liu, H.; Huang, Y.; Zhang, Y.; Chen, X. Co-Delivery of Doxorubicin and Paclitaxel by PEG-Polypeptide Nanovehicle for the Treatment of Non-Small Cell Lung Cancer. *Biomaterials* **2014**, *35*, 6118−6129.
(53) Olson, R. D.; Mushlin, P. S.; Brenner, D. E.; Fleischer, S.; Cusack, B. J.; Chang, B. K.; Boucek, R. J., Jr. Doxorubicin Cardiotoxicity May be Caused by Its Metabolite, Doxorubicinol. *Proc. Natl. Acad. Sci. U. S. A.* **1988**, *85*, 3585−3589.
(54) Cortesi, E.; Aschelter, A. M.; Gioacchini, N.; Pellegrini, A.; Frati, L.; Ficorella, C.; Mazzei, N.; Marchetti, P. Efficacy and Toxicity of 5-Fluorouracil and Folates in Advanced Colon Cancer. *J. Chemother.* **1990**, *2*, 47−50.

DOI: 10.1021/am509204u
ACS Appl. Mater. Interfaces 2015, 7, 6661−6673